JOURNAL OF COLLOID AND INTERFACE SCIENCE 169, 161–167 (1995)

Evanescent Wave Spectroscopic Studies of Surface Enhanced Fluorescence Quantum Efficiencies

ANDREW J. DE MELLO, BEN CRYSTALL, AND GARRY RUMBLES[1]

Department of Chemistry, Imperial College of Science, Technology & Medicine, Exhibition Road, London SW7 2AY, United Kingdom

Received February 1, 1994; accepted June 8, 1994

The techniques of evanescent wave induced fluorescence spectroscopy (EWIFS) and time-correlated single-photon counting have been combined to investigate the photophysical properties of auramine-O at a solid/solution interface. Interaction of the dye with the surface causes an enhancement of the fluorescence quantum efficiency through the restriction of intramolecular rotations. The fluorescence kinetics of the adsorbed molecules are shown to be a function of surface and bulk solution concentration. The application of the maximum entropy method to the analysis of EWIFS decays is also introduced and discussed.

INTRODUCTION

Recently much attention has been focused on the study of molecular interactions and dynamics at interfaces. This is primarily due to their fundamental importance in many areas of chemistry and physics (1, 2).

One technique that has been used to probe interfacial phenomena is evanescent wave induced fluorescence spectroscopy (EWIFS) (3–6). EWIFS utilizes total internal reflection geometry to generate a surface-specific, electromagnetic field disturbance at the interface between two dielectric media. This disturbance exists in the less dense medium and is termed an evanescent wave. Subsequently, the evanescent wave is used to selectively, excite fluorophores in the interfacial region (within ~500 nm of the interface).

The evanescent wave induced fluorescence intensity, I_f, can be described as

$$I_f \propto \int_0^\infty \phi_f(x)c(x)I_0\exp(-x/\Lambda)dx, \qquad [1]$$

where ϕ_f is the fluorescence quantum efficiency of the fluorophore, x is the distance from the interface, $c(x)$ is the fluorophore concentration profile, I_0 is the intensity of the evanescent wave at $x = 0$, and Λ is the penetration depth of the evanescent wave. Therefore, if $\phi_f(x)$ is constant, evanescent wave induced fluorescence intensity measurements directly relate to surface concentrations.

We have combined EWIFS with the method of time-correlated single photon counting (TCSPC) to extend the technique into the time domain.[7] This allows variations in the photophysical properties of an interfacial species to be detected through changes in the form of its fluorescence decay profile. The fluorescence quantum yield of a fluorophore is defined by

$$\phi_f = \frac{k_r}{k_r + k_{nr}} = k_r\tau_f, \qquad [2]$$

where k_r is the radiative deactivation rate constant, k_{nr} is the nonradiative deactivation rate constant, and τ_f is the fluorescence lifetime. Assuming that k_r is independent of environment, then Eq. [1] can be rewritten as

$$I_f = k_r \int_0^\infty \tau_f(x)c(x)I_0\exp(-x/\Lambda)dx. \qquad [3]$$

This refinement of the technique enables:

(i) changes in the fluorescence quantum yield of a species to be detected, through measurement of τ_f and knowledge of k_r; and

(ii) interfacial concentrations to be directly calculated from evanescent wave induced fluorescence intensity measurements.

It has been demonstrated previously that the surface can effect dramatic changes on quantum efficiencies of fluorophores in the interfacial region. An EWIF study of the soluble polydiacetylene poly(4BCMU) indicated adsorption of the polymer onto a fused silica surface. This adsorption process is accompanied by a reduction in the nonradiative deactivation rate constant and an increase in the fluorescence decay time (8). A similar effect had also been observed for the triphenylmethane dye, malachite green. Adsorption of the molecule onto a glass surface restricts the out-of-plane motions responsible for the efficient nonradiative deactivation mechanism, therefore leading to a significant lengthening of

[1] To whom correspondence should be addressed.

0021-9797/95 $6.00

the singlet-state lifetime (9). Conversely, the surface can act to enhance nonradiative deactivation pathways. Both di- and tetrasulphonated aluminium phthalocyanine dyes exhibit a quenched fluorescence decay time when in the vicinity of a fused silica surface. This quenching effect can be switched on and off by the variation of solvent characteristics (6, 10).

Although it is clear that the surface can induce changes in the photophysical properties of molecules, the nature of these changes is not fully understood. The adsorption of a molecule onto a surface will result in a diversity of interactions between the surface and other molecules (11). Even a relatively homogeneous surface will provide a variety of "interfacial environments" for the molecule. Therefore, the sum of all the interactions which add to the radiative and nonradiative decay pathways should yield a distribution of fluorescence lifetimes. This picture is intuitively appealing, and is further supported by the fact that the majority of decays measured in the vicinity of a surface deviate from simple exponential kinetics (12).

Lifetime distribution analysis (LDA) provides a significant improvement on existing fitting routines (13). It allows the differentiation of systems obeying a decay law made up of two or three discrete components from systems where a continuous distribution of lifetime exists. Therefore LDA, in theory, offers the possibility of reconstructing the true shape of fluorescence decays originating from "interfacial environments."

However, the application of this analysis technique to interfacial systems is relatively new and beset by significant problems. The motivation for the current study is to extend this understanding of interfacial phenomena through the investigation of the photophysical properties of the diphenylmethane dye, auramine-O (AO). EWIFS is used to probe the dye in the vicinity of a solid/solution interface. Preliminary data are presented to illustrate surface enhanced fluorescence processes, and the complexity of the fluorescence decay profiles is investigated and discussed, using a variety of analysis techniques.

MATERIALS AND METHODS

Auramine-O monochloride (Aldrich) was recrystallized twice from 0.02 M NaCl at 25°C. Aqueous solutions were made using doubly distilled water (Elgastat UHQ purified). The molar extinction coefficient of AO in water was assumed to be $4.41 \times 10^4\ M^{-1}\ cm^{-1}$ at 430 nm. For EWIF spectroscopic measurements the sample was contained in a modified cuvette which allowed the solution to contact the surface of a hemispherical prism (Spanoptic, $n_1 = 1.46$). The AO solutions were assumed to have a refractive index of 1.34 at 430 nm (i.e., that of water). The prism then acts as the internal reflection element generating the evanescent wave in the solution. The prism surface was cleaned prior to each experiment by treatment with concentrated sulphuric acid and water.

Fluorescence decays were recorded using a TCSPC system, equipped with an EWIF spectrometer assemblage. Full details of the system will be described elsewhere. Briefly, the excitation light was provided by a cavity-dumped stilbene-3 dye laser (Coherent 590 CD/7220), synchronously pumped by the third harmonic of a mode-locked Nd:YAG laser (Coherent Antares 76-s). This produced a 3.8-MHz pulse train at 430 nm. The detection system consisted of a 0.22-m single monochromator (Spex 1681), microchannel-plate photomultiplier (Hamamatsu R1564U-07), constant fraction discriminator (Ortec 584), time-to-amplitude converter (Ortec 547), and a multichannel pulse-height analyzer (Tennelec PCA2). Steady-state EWIF measurements were performed on a similar EWIF spectrometer system. Here excitation was provided by the 457.9-nm line of a cavity dumped argon-ion laser (Spectra Physics 164). Under the present experimental conditions, the critical angle for total internal reflection was approximately 65.6°.

Fluorescence decays were collected to 20,000 counts in the channel of maximum intensity. Decays were analyzed using two methods:

Method 1: Sum of exponentials. Decays were analyzed as a sum of up to three exponentials, using a normal iterative, reconvolution routine based on the Marquardt algorithm (14). Both exponentials and lifetimes are variable parameters of the fitting routine.

Method 2: Lifetime distribution analysis. The maximum entropy method (MEM) was utilized to obtain the underlying lifetime distribution from the EWIF decay. The method assumes 100 exponents with fixed, logarithmically spaced lifetimes.

Fluorescence emission spectra were obtained using a Spex FluoroMax single photon counting spectrometer. The bandpass of both excitation and emission slits was 0.6 nm, and spectra were corrected for variations in lamp intensity.

Absorption spectra were recorded on a Perkin–Elmer Lambda 2 spectrophotometer, using a standard 10-mm-pathlength cell.

RESULTS

Figure 1 shows selected bulk fluorescence emission spectra of AO in water. Part (a) describes emission excited at 430 nm. It is observed that the fluorescence spectrum is distorted by a narrow band occurring at approximately 510 nm. Figure 1b describes emission excited at 458 nm. The spectrum is now distorted by a shoulder at approximately 545 nm. The origin of this distortion is the symmetric stretching Raman mode of water ($\Delta\nu \approx 3650\ cm^{-1}$). The existence of this distortion demonstrates the very low fluorescence quantum efficiency of AO in free solution. The deconvoluted emission spectrum is shown in Fig. 1c to illustrate the true shape of the fluorescence emission.

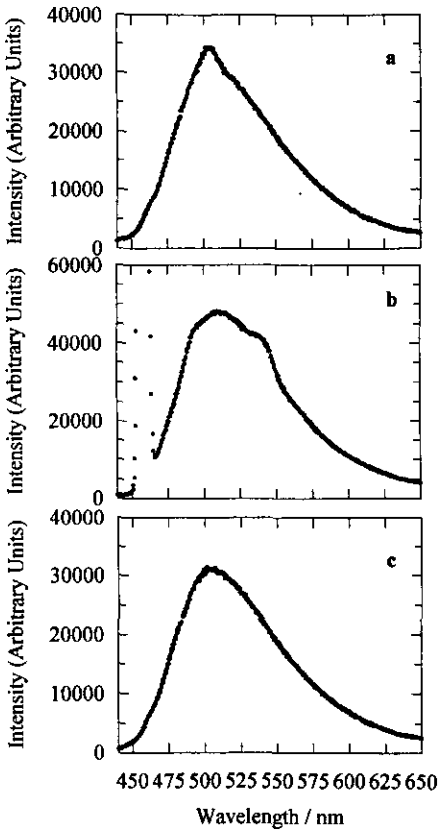

FIG. 1. Bulk fluorescence emission spectra of AO in water (10^{-5} mol dm^{-3}): (a) excitation wavelength = 430 nm; (b) excitation wavelength = 457.9 nm; (c) deconvoluted fluorescence emission spectrum (Raman scatter contribution removed).

A molecule in its first excited state can return to the ground state via radiative or nonradiative pathways. Nonradiative transitions are normally ascribed to the transfer of excited state energy to vibrational energy of the ground state. The vibrational energy is then transferred to the surroundings as heat. Diphenylmethane dyes, such as AO, possess an alternative deactivation pathway. In a free environment, large torsional motions of the two degenerate Ph-$(CH_3)_2$ groups around the central C atom allow excited state energy to be dissipated through nonradiative pathways. Therefore, in aqueous solution internal rotations dominate the deactivation pathways, and the fluorescence quantum efficiency of AO is very low (15).

Figure 2 shows an EWIF spectrum of AO in water at a glass surface ($\Lambda \sim 100$ nm). It is observed that the spectral profile is identical to the deconvoluted bulk emission spectrum, and visual inspection of the EWIF spot indicates a dramatic increase in fluorescence intensity. Alone, these two observations imply that either (a) the fluorescence quantum efficiency of the dye increases in the vicinity of the interface or (b) the interfacial concentration of dye molecules is much larger than the bulk concentration. To establish the real reason for the observed intensity increase, time-resolved measurements were made. Since $\phi_f \propto \tau_f$ (Eq. [2]), the bulk fluorescence quantum efficiency can be related to the interfacial fluorescence quantum efficiency through comparison of the fluorescence decaytimes. Figure 3a represents the bulk fluorescence decay of AO in water. With the current apparatus the decay was almost indistinguishable from the instrument response function (FWHM $\sim$ 80 ps), and was satisfactorily described by a single exponential decay function of 9 ps. A better description of the decay is obtained using a biexponential fit (τ_1 = 3 ps, $A_1 = 99.9/\tau_2$ = 400 ps, A_2 = 0.1). The radiative lifetime of AO was calculated (from ab-

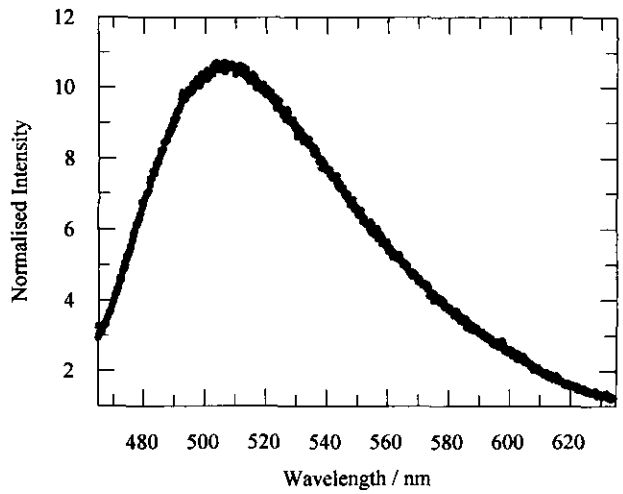

FIG. 2. Evanescent wave induced fluorescence spectrum of AO at a glass/water interface. Bulk solution concentration = 10^{-5} mol dm^{-3}, Λ = 80 nm, and excitation wavelength = 457.9 nm.

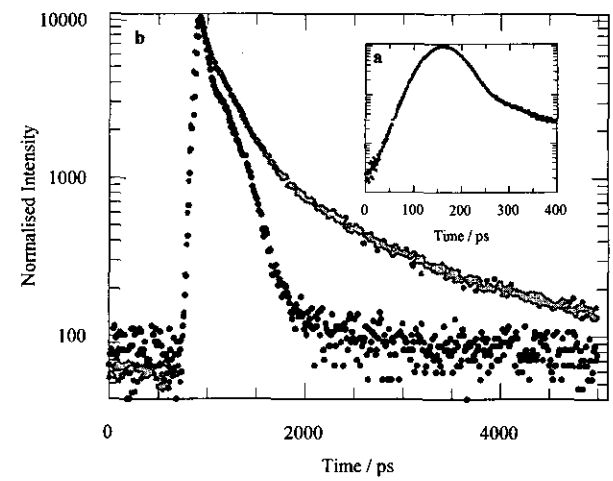

FIG. 3. (a) Fluorescence decay profile of AO in water (10^{-5} mol dm^{-3}). (b) Evanescent wave induced fluorescence decay profile of AO at a glass/water interface (instrument response function ~80 ps FWHM). Bulk solution concentration = 10^{-5} mol dm^{-3}, Λ = 80 nm, and excitation wavelength = 430 nm.

sorption measurements) to be approximately 3 ns, using the Strickler–Berg relationship (16). Therefore, according to Eq. [2], the fluorescence quantum efficiency of AO in bulk solution was estimated to be ~0.003.

Figure 3b represents the time-resolved EWIF decay of AO at a glass surface. It can be seen that the singlet-state decay time has been lengthened to yield an average lifetime of 260 ps. Hence, the observed increase in fluorescence is predominantly a consequence of an increase in the fluorescence quantum efficiency of AO in the interfacial region. This increase is attributed to surface–molecule and molecule–molecule interactions inhibiting the torsional motions responsible for deactivation by internal rotations.

The penetration depth of the evanescent wave is defined as the distance required for the amplitude of the evanescent wave to be attenuated to $1/e$ of its boundary value, and can be mathematically approximated as

$$\Lambda \approx \frac{\lambda}{4\pi n_1}\left\{\frac{1}{\sin^2\theta_i - (n_2/n_1)^2}\right\}^{1/2}, \qquad [4]$$

where λ is the wavelength of incident light, θ_i is the incident angle, n_1 is the refractive index of prism, and n_2 is the refractive index of the sample (3). Therefore the depth probed by the evanescent wave can be varied through changes in θ_i. Subsequently Λ was varied (between 50–150 nm) and decays were measured. No change in the decay profile was detected, indicating that the evanescent wave induced fluorescence originates from a region which is small with respect to the penetration depth. Hence, the existence of a thin adsorbed dye layer is probable. This confirms that the inhibition of the torsional motions is predominantly a surface phenomenon. Further studies are currently in progress to establish the adsorbed layer thickness.

The complexity of the interfacial environment is demonstrated by the heterogeneity of the EWIF decay, which can only be successfully parameterized by a triexponential decay function ($\tau_1 \sim 60$ ps, $\tau_2 \sim 400$ ps, $\tau_3 \sim 1700$ ps; $\chi^2 \sim 1.4$). In general, the number of measured lifetimes that result from a sum of exponentials analysis reflects the number of noninteracting species contributing to the decay. On this basis there are three distinct auramine-O species in the interfacial region. All components are significantly longer than the bulk fluorescence decaytime, indicating that the evanescent wave induced fluorescence originates from species which are spatially confined to some extent. The short component describes species which are loosely interacting with the surface, the middle component describes species which are more strongly interacting, and the longest component represents species which are irreversibly associated with the surface (on the time scale of the experiment). Nevertheless, the quality of the exponential fits ($1.3 < \chi^2 < 1.8$; $1.7 <$ DW < 2.0) suggests that the resulting lifetimes may simply represent an average of the AO species that really exist in the interfacial region.

Since the bulk solution fluorescence decay kinetics appear to be relatively simple, the apparent complexity in the EWIF decay must be a consequence of the surface and/or the concentration of surface species. To investigate the effect of surface concentration, a "concentration series" was performed. Solution was allowed to adsorb to the prism surface for 2 h. Bulk solution was then replaced by fresh solvent and the system allowed to equilibrate for 20 min. This process was repeated a number of times, with an EWIF decay being measured prior to each solvent flush. The three decays are illustrated in Fig. 4. It is observed that "washing" the surface leads to an increase in the decaytime of the molecule. If the idea of three noninteracting species is correct, then washing the surface should only change the relative yields of each component; the individual lifetimes will remain constant. Hence, the decays were analyzed globally, where three lifetimes common to all decays were calculated (17).

The results given in Table 1 demonstrate three common lifetimes of 55, 396, and 1574 ps. The relative yield of the long lifetime component increases with washing, while the relative yield of the short lifetime component decreases. This is reflected by a general lengthening in the EWIF decay time. The origin of this progression is twofold. First, the process of "surface washing" induces the removal of loosely associated surface molecules from the interfacial region. The "effective" concentration of the strongly associated species in the interfacial region therefore increases. This increase manifests itself as a lengthening of the EWIF decay time. Second, high surface concentrations facilitate efficient energy transfer between adsorbed species (18). This leads to the quenching of fluorescence within the adsorbed layer. Since

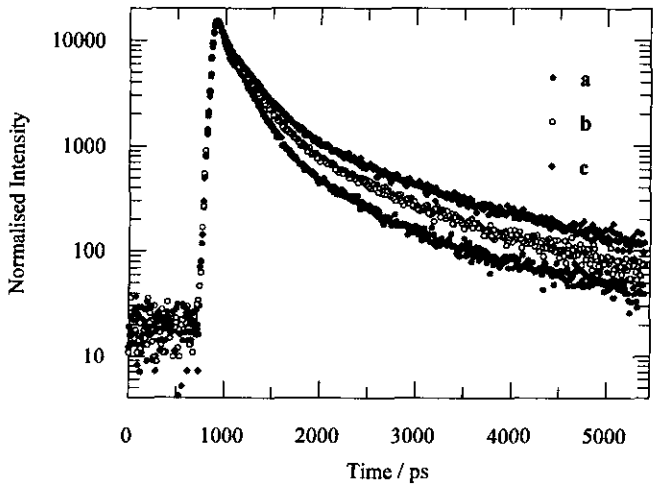

FIG. 4. Evanescent wave induced fluorescence decay profiles of AO at a glass/water interface. (a) Bulk solution concentration = 10^{-5} mol dm^{-3}, Λ = 80 nm, and excitation wavelength = 430 nm; (b) after 2 "surface washes"; (c) after 5 "surface washes."

TABLE 1

Variation in the Relative Yield of Each Lifetime Component of the EWIF Decay as a Function of the Concentration of Surface-Associated Species

Experimental conditions	Yield (%)			Average τ (ps)
	τ_1 = 55 ps	τ_2 = 396 ps	τ_3 = 1574 ps	
Bulk solution	71.1	20.2	08.7	260
Wash 1	64.7	23.0	12.3	320
Wash 2	56.7	25.0	17.3	410
Wash 3	51.1	27.4	21.5	470
Wash 4	47.6	27.1	25.3	530
Wash 5	43.4	26.2	30.4	610

quenching is dependent on the number of adsorbed molecules per unit area, washing will diminish the probability of quenching, and thus lengthen the observed decaytime.

Investigations into the effect of the surface on the decay are currently being performed. The behavior of AO in water (10^{-4}–10^{-8} M) near modified glass and PMMA surfaces demonstrates interesting properties. Qualitatively, it is apparent that the surface does play a role in determining the form of the EWIF decay. Variations in the decay form are observed. These results will be discussed in detail in a subsequent communication.

As stated the "sum of exponentials" global analysis yielded the following decay law for AO in water at a glass surface:

$$I(t) = A_1\exp(-t/\tau_1) + A_2\exp(-t/\tau_2) + A_3\exp(-t/\tau_3), \quad \sum_{i=1}^{N} A_i = 1. \quad [5]$$

Here $I(t)$ is the decay intensity at time t, τ_1 = 55 ps, τ_2 = 396 ps, and τ_3 = 1547 ps. Nevertheless, it has been established that acceptable 2- and 3-component fits can conceal underlying lifetime distributions (13). Therefore, the EWIF decays were analyzed using the MEM. Decays reconstructed from the MEM are free from the artifactual correlations inherent in conventional iterative reconvolution routines. No assumptions about the model are made until the lifetime pattern is mapped out.

As observed, AO molecules adsorbed to a glass surface possess complex decay characteristics. This is consistent with a model describing a set of independent emitters, with lifetimes distributed in some manner. Therefore, a probe function can be represented by the sum

$$I(t) = \sum_{i=1}^{100} a_i\exp(-t/\tau_i), \quad [6]$$

i.e., 100 fixed, logarithmically spaced lifetimes (τ_i) between 10 and 10,000 ps. Reconstruction of the amplitudes (a_i) is achieved by maximizing the *entropy-like* function (19, 20)

$$S = -\sum_{i=1}^{100} a_i \ln\{a_i / \sum_{i=1}^{100} a_i\}. \quad [7]$$

The MEM-recovered lifetime distributions from two EWIF decays are shown in Fig. 5. Part (a) represents low surface concentration, and part (b) represents high surface concentration. It is observed that both decays do not yield three discrete lifetimes but a broad distribution of lifetimes. Qualitatively, this is not surprising. As noted, the interfacial environment is one of significant heterogeneity. The dye molecules can be imagined as associating with the surface through electrostatic and hydrophobic interactions. The surface is not uniform on a microscopic scale, and will provide a variety of binding sites. This variation along with the added effect of solute–solute interactions will intuitively yield a continuous distribution of lifetimes. It is noted that both distributions are bimodal, with local maxima at 40–70 and 600–700 ps. At high surface coverages the individual maxima of the distribution are shifted to shorter lifetimes compared to the maxima at low surface coverage distributions. This is consistent with the sum-of-exponential analysis, where the average decay time increases with decreasing surface concentration (and bulk concentration). This effect, as noted, is a consequence of high surface concentrations facilitating efficient energy transfer between adsorbed species.

To further investigate the significance of the shape of the distributions synthetic decay curves were generated from the impulse decay function

$$D(t) = \sum_{i=1}^{N} a(i)\exp[-t/\tau(i)]. \quad [8]$$

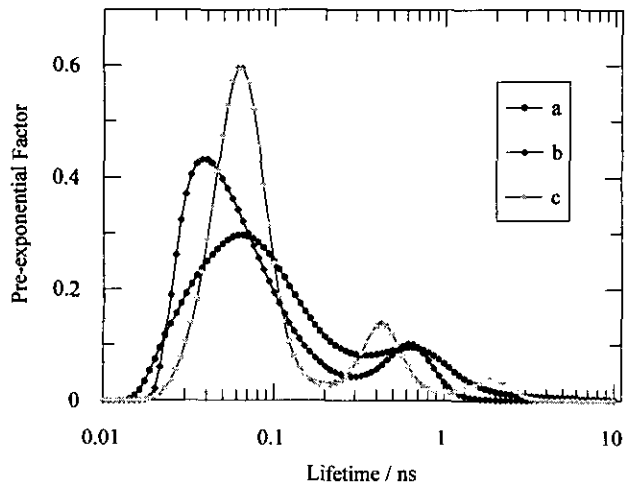

FIG. 5. MEM analysis of fluorescence decays: (a) EWIF decay illustrated in Fig. 4a; (b) EWIF decay illustrated in Fig. 4c; (c) simulated decay constructed from a "true" triexponential decay law (τ_1 = 55 ps, τ_2 = 400 ps, and τ_3 = 1700 ps). Probe function of 100 terms over 10–10,000 ps, fitting range of 400 channels (11.4 ps/channel).

Here $D(t)$ is the decay intensity at time t, $a(i)$ is the preexponential assigned to the lifetime $\tau(i)$, and N is the number of exponentials describing the decay. An experimentally determined instrument response function (IRF) having 20,000 counts in the channel of maximum intensity was subsequently used to generate a convolved decay curve $C(t)$,

$$C(t) = \int_0^\infty f(s)D(t-s)ds, \qquad [9]$$

where $f(s)$ is the IRF. The simulated decays were scaled to 20,000 counts in the channel of maximum intensity, and Gaussian noise was added to approximate Poisson counting statistics (21).

Triexponential, convoluted decays were generated to precisely describe the results indicated in Table 1. These decays were then analyzed using the MEM to generate the lifetime distributions resulting from "true" triexponential decays. A representative distribution is shown in Fig. 5c. It is observed that the distribution is trimodal, with the maxima of each Gaussian, being described by the individual lifetimes obtained from the sum-of-exponentials analysis (i.e., ~55, 400, and 1700 ps). This demonstrates that a true triexponential decay will yield a well defined trimodal distribution. Therefore, the triexponential description of the EWIF decays which were previously used, can only be an approximation of reality and provide qualitative information. However, the MEM analysis reveals a hidden complexity in the interfacial environment which can easily be overlooked.

DISCUSSION

Spectroscopic measurements of AO in solution demonstrate an extremely low fluorescence quantum yield ($\phi_F \sim 0.003$). Steady-state fluorescence emission is weak and distorted by the symmetric Raman stretching mode of the solvent. The fluorescence decay of AO in water is short, and can be approximated by a single lifetime of approximately 9 ps. However, the temporal kinetics are more precisely described by a biexponential decay. This behavior is consistent with the barrierless relaxation model proposed by Vogel *et al.* (22). As stated, in the excited state AO molecules undergo rapid conformational change through rotation of both phenyl rings around the central carbon atom. The rotations do not possess an activation barrier and are facilitated by a driving force imparted by the gradient of the excited state hypersurface. This gradient itself is dependent on the viscosity of the immediate environment. Therefore, in high viscosity media the gradient of the excited state hypersurface will be lowered and deactivation via internal rotations will be reduced. Steady-state emission measurements of AO in alcoholic solvents demonstrate this phenomenon. As solvent viscosity is increased there is a marked enhancement of the fluorescence quantum yield. This increase can be generally ascribed to the inhibition of internal rotations (10).

EWIF spectroscopic studies of AO in water near a glass surface demonstrate a significant enhancement of fluorescence emission. Steady-state emission is intense and no distortion due to Raman scatter is detected in EWIF spectra. Time-resolved measurements yield a complex decaytime which is significantly longer than the bulk decaytime. Hence, the increase in fluorescence is predominantly a consequence of an enhanced fluorescence quantum efficiency near the surface. The increase in the fluorescence quantum efficiency is rationalized in terms of inhibition of the barrierless rotations, through interaction of the fluorophore with the surface. Thus, deactivation of the excited state occurs through more radiative pathways. Complexity is introduced into the decay because of the heterogeneity of the interfacial environment.

The time-resolved measurements demonstrate important effects. Firstly, development of EWIFS as a sensitive surface analysis technique, relies on the ability to quantitate surface bound species. Use of Eq. [1] to calculate $c(x)$ requires an exact knowledge of $\phi_f(x)$. Since the interfacial decays obtained are complex, a single exponential lifetime cannot be used to describe the profile. Therefore, an average lifetime is constructed from the components of the decay. These are listed in Table 1. Although this is a simplification, it provides an approximation of the modified quantum efficiency of the fluorophore near a surface. Hence, $c(x)$ can be estimated with greater confidence.

Second, the interfacial kinetics pose some interesting questions. The MEM analysis of the EWIF decays reveals significant interfacial heterogeneity. All decays are complex and do not correspond to lifetime distributions resulting from synthetic, triexponential decays. But what does the shape of the lifetime distribution tell us? From this initial study, it is apparent only that the EWIF decays are constructed from a broad distribution of emitters, and not three noninteracting fluorescent species (as indicated by nonlinear, least-squares iterative reconvolution routine). The nature of the surface–molecule interactions appears to be critical in determining the shape of the lifetime distribution, and further studies are currently in progress to investigate these effects. However, it is noted that the triexponential decay model does provide a good working approximation, and can be successfully used to obtain qualitative information about the interfacial environment.

Briefly, it is also recognized that the assumption used to validate Eq. [3] (i.e., that k_r is independent of environment) is not strictly correct. Previously, it has been shown that k_r has a dependence on the refractive index of the local environment:

$$k_r \propto n^2 \int \left(\frac{\epsilon(\nu)}{\nu}\right) d\nu. \qquad [10]$$

Here, the integrated term describes the area under the absorption spectrum of an emitting chromophore (23). The significance of this relationship may be heightened when the chromophore is located in the immediate vicinity of the solid/solution boundary. For example, in the current study adsorption of AO molecules may modify the local dielectric function very close to the glass surface. It has also recently been demonstrated that the solid/liquid interface can influence the relaxation of a point dipole on the liquid side. These calculations assume a nonlocal dielectric function (24, 25). However, it is expected that any variations in k_r should be relatively small in most physical systems.

CONCLUSIONS

The techniques of EWIFS and TCSPC have been successfully combined to study the spectral and temporal photophysics of auramine-O in the vicinity of a glass/water interface. The ability to differentiate between surface-adsorbed and bulk-solvated dye on the basis of emission kinetics has been achieved. Results demonstrate that the interaction of the surface with solute molecules leads to a significant modification of the fluorescence quantum efficiency. This modification is a function of bulk solution and surface concentration.

The application of the MEM of decay analysis has illustrated the complexity of EWIF decays and thus the heterogeneity of the interfacial environment. This novel application of the MEM to EWIF decays, although in its early stages, offers the possibility of revealing hidden complexity, and obtaining physical significance from fluorescence decays originating from interfacial regions.

ACKNOWLEDGMENTS

The authors thank the Science and Engineering Research Council (SERC, United Kingdom) for financial support for this work. AJD thanks Kodak, Ltd. for a SERC Case Studentship. The authors are also grateful to V. C. Arunasalam and M. Carey for their help and useful discussions.

REFERENCES

1. MacRitchie, F., "Chemistry at Interfaces." Academic Press, San Diego, 1990.
2. Horbett, T. S., and Brash, J. (Eds.), "Proteins at Interfaces" Amer. Chem. Soc. Symp. Series, vol. 343, Amer. Chem. Soc., Washington, DC, 1987.
3. Toriumi, M., and Masuhara, H., *Spectrochim. Acta Rev.* **14,** 353 (1991).
4. Reichert, W. M., *Crit. Rev. Biocompat.* **5,** 173 (1989).
5. Hlady, V., Reinecke, D. R., and Andrade, J. D., *J. Colloid Interface Sci.* **111,** 555 (1986).
6. Rumbles, G., Brown, A. J., and Phillips, D., *J. Chem. Soc. Faraday Trans.* **87,** 825 (1991).
7. O'Connor, D. V., and Phillips, D., "Time-Correlated Single-Photon Counting." Academic Press, London, 1985.
8. Rumbles, G., Brown, A. J., Phillips, D., and Bloor, D., *J. Chem. Soc. Faraday Trans.* **88,** 3313 (1992).
9. Bell, M., Crystall, B., Rumbles, G., Klug, D. R., and Porter, G., unpublished results.
10. de Mello, A. J., and Rumbles, G., unpublished results.
11. Francis, C., Lin, J., and Singer, A., *Chem. Phys. Lett.* **94,** 162 (1983).
12. James, D. R., Lin, Y., DeMayo, P., and Ware, W. R., *Chem. Phys. Lett.* **120,** 460 (1985).
13. James, D. R., and Ware, W. R., *Chem. Phys. Lett.* **126,** 7 (1986).
14. Janot, J. M., Beeby, A., Bayley, P. M., and Phillips, D., *Biophys. Chem.* **41,** 277 (1991).
15. Oster, G., and Nishijima, Y., *J. Am. Chem. Soc.* **78,** 1581 (1956).
16. Strickler, S. J., and Berg, R. A., *J. Chem. Phys.* **37,** 814 (1962).
17. Knutsen, J. R., Beecham, J. M., and Brand, L., *Chem. Phys. Lett.* **102,** 501 (1983).
18. Förster, T., *Ann. Phys.* **2,** 55 (1948).
19. Smith, C. R., and Grady, W. T., Jr. (Eds.), "Maximum Entropy and Bayesian Methods in Inverse Problems." Reidel, Boston, 1985.
20. Siemiarczuk, A., Wagner, B. D., and Ware, W. R., *J. Phys. Chem.* **94,** 1661 (1990).
21. Carey, M., and Smith, T. A., personal communication.
22. Vogel, M., and Rettig, W., *Ber. Bunsenges. Phys. Chem.* **91,** 1241 (1987).
23. Hirayama, S., and Phillips, D., *J. Photochem.* **12,** 139 (1980).
24. Urbakh, M., and Klafter, J., *J. Phys. Chem.* **96,** 3480 (1992).
25. Urbakh, M., and Klafter, J., *J. Phys. Chem.* **97,** 3344 (1993).